



HAL
open science

When Metal Complexes Evolve, and a Minor Species Is the Most Active: the Case of Bis(Phenanthroline)Copper in the Catalysis of Glutathione Oxidation and Hydroxyl Radical Generation

Enrico Falcone, Vincenzo Vigna, Hemma Schueffl, Francesco Stellato, Bertrand Vileno, Merwan Bouraguba, Gloria Mazzone, Olivier Proux, Silvia Morante, Petra Heffeter, et al.

► To cite this version:

Enrico Falcone, Vincenzo Vigna, Hemma Schueffl, Francesco Stellato, Bertrand Vileno, et al.. When Metal Complexes Evolve, and a Minor Species Is the Most Active: the Case of Bis(Phenanthroline)Copper in the Catalysis of Glutathione Oxidation and Hydroxyl Radical Generation. *Angewandte Chemie International Edition*, 2024, 10.1002/anie.202414652 . hal-04774796v1

HAL Id: hal-04774796

<https://hal.science/hal-04774796v1>

Submitted on 8 Nov 2024 (v1), last revised 29 Nov 2024 (v2)

HAL is a multi-disciplinary open access archive for the deposit and dissemination of scientific research documents, whether they are published or not. The documents may come from teaching and research institutions in France or abroad, or from public or private research centers.

L'archive ouverte pluridisciplinaire **HAL**, est destinée au dépôt et à la diffusion de documents scientifiques de niveau recherche, publiés ou non, émanant des établissements d'enseignement et de recherche français ou étrangers, des laboratoires publics ou privés.

When Metal Complexes Evolve, and a Minor Species Is the Most Active: the Case of Bis(Phenanthroline)Copper in the Catalysis of Glutathione Oxidation and Hydroxyl Radical Generation

Enrico Falcone,^{[a],‡,#} Vincenzo Vigna,^{[b],#} Hemma Schueffl,^[c] Francesco Stellato,^{[d],[e]} Bertrand Vileno,^[a] Merwan Bouraguba,^[a] Gloria Mazzone,^[b] Olivier Proux,^[f] Silvia Morante,^{[d],[e]} Petra Heffeter,^[c] Emilia Sicilia,^{[b],#*} Peter Faller^{[a],g,#*}

^[a] Dr. E. Falcone, Dr. B. Vileno, M. Bouraguba, Prof. P. Faller
Institut de Chimie (UMR 7177)
University of Strasbourg, CNRS
4 Rue Blaise Pascal, 67081 Strasbourg, France
Email: pfaller@unistra.fr

^[b] V. Vigna, Dr. G. Mazzone, Prof. E. Sicilia
Department of Chemistry and Chemical Technologies
Università della Calabria
87036 Arcavacata di Rende (CS), Italy
Email: emilia.sicilia@unical.it

^[c] H. Schueffl, Prof. P. Heffeter
Center for Cancer Research and Comprehensive Cancer Center
Medical University of Vienna, 1090 Vienna, Austria

^[d] Prof. F. Stellato, Prof. S. Morante
Department of Physics
Università di Roma Tor Vergata
Via della Ricerca Scientifica 1, 00133 Roma, Italy

^[e] Prof. F. Stellato, Prof. S. Morante INFN, Sezione di Roma Tor Vergata
Via della Ricerca Scientifica 1, 00133 Roma, Italy

^[f] Dr. O. Proux
Observatoire des Sciences de l'Univers de Grenoble, UAR 832
CNRS-Université Grenoble Alpes
38041 Grenoble, France

^[g] Prof. P. Faller
Institut Universitaire de France (IUF)
1 rue Descartes, 75231 Paris, France

‡ current address: Laboratoire de Chimie de Coordination (UPR 8142), CNRS, 31077 Toulouse, France

These authors contributed equally

Abstract

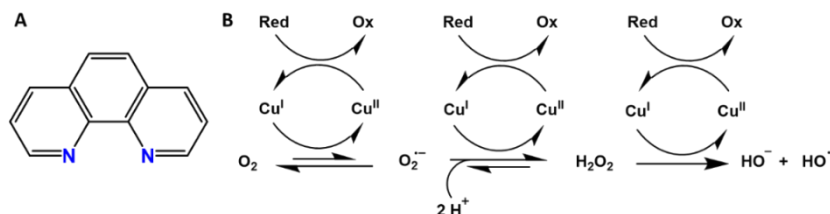
Several copper-ligands, including 1,10-phenanthroline (Phen), have been investigated for anticancer purposes based on their capacity to bind excess copper (Cu) in cancer tissues and form redox active complexes able to catalyse the formation of reactive oxygen species (ROS), ultimately leading to oxidative stress and cell death. Glutathione (GSH) is a critical compound as it is highly concentrated intracellularly and can reduce and dissociate copper(II) from the ligand forming poorly redox-active copper(I)-thiolate clusters. Here we report that Cu-Phen₂ speciation evolves in physiologically relevant GSH concentrations. Experimental and computational experiments suggest that at pH 7.4 mostly copper(I)-GSH clusters are formed, but a minor species of copper(I) bound to one Phen and forming ternary complexes with GSH (GS-Cu-Phen) is the redox active species, oxidizing quite efficiently GSH to GSSG and forming HO[•] radicals. This minor active species becomes more populated at lower pH, such as typical lysosomal pH 5, resulting in faster GSH oxidation and HO[•] production. Consistently, cell culture studies showed lower toxicity of Cu-Phen₂ upon inhibition of lysosomal acidification. Overall, this study underscores that sub-cellular localisation can considerably influence the speciation of Cu-based drugs and that minor species can be the most redox- and biologically- active.

Keywords

bioinorganic chemistry; copper complex; ternary complex; reactive oxygen species

Introduction

Owing to its role in fundamental biochemical processes (e.g. cellular respiration, collagen formation, neurotransmitter biosynthesis, etc.), copper (Cu) is an essential element for humans.^[1] This is probably best proven by the poor life expectancy (< 4 years) of children affected by Menkes' disease, a genetic disorder of Cu metabolism characterised by systemic Cu deficiency.^[2] On the contrary, cancer cells and tumour tissues show increased Cu levels, which promote cell growth and proliferation (cuproplasia), for instance via the activation of the MAPK pathway, and the development of metastasis through the remodelling of the extracellular matrix by the Cu-dependent enzyme lysyl oxidase (LOX).^[3-6] Nevertheless, excess Cu is toxic to cells. Lately, anticancer Cu-ionophores such as elesclomol and disulfiram have been shown to induce a Cu-dependent form of regulated cell death, called cuproptosis, characterized by lipoylated protein aggregation.^[7] Thus, Cu accumulation in cancer tissues could be exploited for improved selectivity of anticancer therapy.^[5,8-15] Besides Cu-ionophores, ligands that bind excess Cu in cancer tissues forming redox-active Cu complexes could be employed to induce cell death via the generation of reactive oxygen species (ROS).^[5,15] In this respect, the bidentate ligand 1,10-phenanthroline (Phen, Scheme 1) and some of its derivatives are of interest, as they form redox-active Cu complexes that are particularly efficient in the catalysis of ROS production fuelled by reductants such as ascorbate and glutathione, GSH (Scheme 1).^[16,17] In this context, Cu-Phen₂ has been postulated as the redox-active species,^[16] although it is also known the ternary GS-Cu-Phen species can be formed.^[18]



Scheme 1. A) Structure of 1,10-phenanthroline (Phen) and B) scheme of Cu-catalysed ROS formation fuelled by a reductant (Red) such as GSH.

Extensive research on Cu-Phen and its derivatives as anticancer agents is ongoing since its ability to induce oxidative damage on DNA was discovered.^[19-21] Remarkably, mixed complexes between Cu^{II}, phenanthroline and amino acids (known as Casiopeinas[®]) have entered Phase I clinical trials.^[22] Moreover, Cu-Phen complexes are able to increase ROS production and the ratio between oxidised and reduced glutathione (GSSG to GSH ratio) in cells.^[23,24] However, the stability of Cu-Phen₂ complexes, and hence their pro-oxidant activity in biological systems, is challenged by the presence of serum albumin in the extracellular medium,^[25] as well as GSH and metallothioneins in most cell compartments, including cytosol and nucleus.^[17] GSH and MTs are thiol-bearing molecules able to reduce Cu^{II} and tightly bind Cu^I and hence they are able to dissociate and de-activate Cu-based drugs, including Cu^{II}-Phen₂.^[17] Moreover, some of us have recently demonstrated that the stability of a class of Cu-based anticancer drugs (i.e. Cu-thiosemicarbazone complexes) against GSH correlates with their ability to generate ROS and their cytotoxicity.^[26,27] Indeed, the Cu^I-GSH clusters formed upon reductive dissociation of the Cu^{II}-complex are relatively inert towards the reduction of dioxygen.^[28,29] These findings question the paradigmatic pro-oxidant and nuclease activity of Cu-Phen₂ *in vivo*. Nevertheless, we reasoned that Cu-Phen₂ might retain higher stability and activity in organelles where the competition for Cu is lower, such as the endoplasmic reticulum, lysosomes or mitochondria, due to the lack of metallothioneins. Lysosomes appear as well-suited candidates since they are not only devoid of metallothioneins, but their acidic pH (4.5 – 5.5) also remarkably decreases the affinity of GSH for Cu^I (see Supporting Information) relative to most cell compartments (cytosol, nucleus). Of note, since the pK_a of Phen is 4.8, it is neutral at pH 7.4, while it becomes positively charged at lysosomal pH. Hence, Phen could enter by passive diffusion through the membrane and then accumulate into lysosomes. In this study, we first provide evidence that Cu^{II}-Phen₂ evolves in physiologically relevant excess of GSH, forming mostly Cu^I-GSH clusters and minor GS-Cu^I-Phen species, that is responsible for the GSH oxidation and HO[·] production. Lowering the pH to 5 increases the population of such a ternary complex and the correlated HO[·] production. Finally, we also provide unprecedented evidence that lysosomal acidification in cancer cells could be crucial for the cytotoxic activity of Cu-Phen₂.

Results and discussion

Higher stability of Cu^{II}-Phen₂ against GSH at lysosomal pH

In order to assess the hypothesis that Cu-Phen₂ maintains greater stability against GSH at acidic pH, we first examined the formation of Cu^I-GSH clusters upon the reaction of Cu^{II}(Phen)₂ with excess GSH at pH 7.4 and 5. In particular, we measured the characteristic low-temperature (77 K) luminescence at ≈425 nm (upon excitation at 310 nm), arising from cluster-centred 3d⁹4s¹→3d¹⁰ transitions in Cu₄(GS)₆ clusters (Figure 1A).^[30–32] Although this measurement provides only semi-quantitative results (due to inhomogeneous sample freezing), it revealed that most Cu^{II} is reductively dissociated from Phen forming Cu^I-GSH clusters at pH 7.4, while only a minor portion (≈30%) is bound to GSH at pH 5 (Figure 1B).

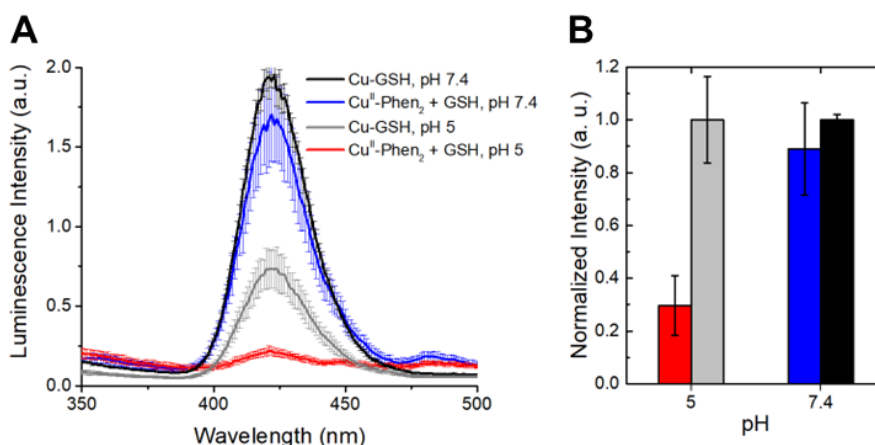


Figure 1. Formation of Cu-GSH clusters monitored by low-temperature (77 K) luminescence. A) Low-temperature luminescence spectra ($\lambda_{\text{ex}} = 310$ nm) of Cu^{II} or Cu^{II}-Phen₂ upon addition of GSH at pH 7.4 or 5. Samples were freeze-quenched in liquid N₂, three spectra were collected upon rotating the sample quartz tube in the liquid N₂ dewar and the standard deviation was calculated on such replicates. B) Luminescence intensity at 422 nm normalized to the intensity of the samples containing Cu^{II} only at each pH. Sample composition: [Cu^{II}] = 10 μ M, [Phen] = 25 μ M, [GSH] = 1 mM, buffer: HEPES 100 mM pH 7.4 or MES 100 mM pH 5.

We further investigated the reaction between Cu^{II}-Phen₂ and GSH by X-ray absorption spectroscopy (XAS), which is sensitive to both Cu redox states and their coordination sphere. In particular, Cu^{II}-Phen₂, Cu^I-Phen₂ (formed by the addition of excess sodium ascorbate) and Cu^I-GSH complexes show different X-ray absorption near-edge spectroscopy (XANES) spectra at both pH 7.4 and 5 (Figure 2). A quantitative analysis of the high-energy region of the spectra, the extended X-ray absorption fine structure (EXAFS), of Cu-Phen₂ and Cu-GSH complexes is provided in the SI (Figures S1-4, Tables S1-3). The XANES spectra of ternary mixtures obtained upon the addition of GSH to Cu^{II}-Phen₂ look different from both Cu-Phen₂ and Cu-GSH binary systems (Figure 2A, B, green curves). The presence of a pre-edge feature around 8983 eV attributed to the 1s→4p transition of monovalent Cu ions, suggests that in these samples Cu is, at least partially, reduced by GSH.^[33] The Fourier Transform (FT) moduli of the EXAFS (which represent a pseudo-radial distribution function) of the ternary mixture at pH 7.4 clearly shows a peak at a distance of about 2.8 Å, which corresponds to the Cu-Cu distance and is therefore an additional indication of the presence of Cu^I-GSH clusters (Figure 2C, green curve). A peak in the same position is indeed present in the Cu-GSH samples, which are characterized by the presence of Cu^I-GSH clusters (Figure 2C, black curve). On the contrary, such a peak is not observed in the ternary mixture at pH 5 (Figure 2D), corroborating the absence (or at least a very low population) of Cu^I-GSH clusters at this pH.

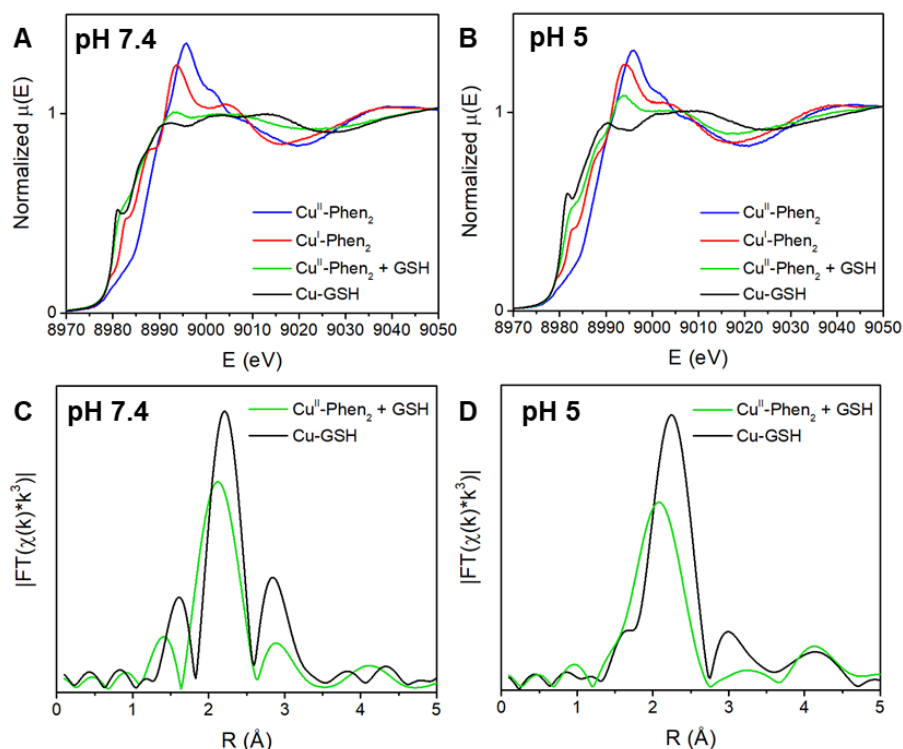


Figure 2. XAS characterization of the reaction between $\text{Cu}^{\text{II}}\text{-Phen}_2$ and GSH. A, B) XANES spectra of $\text{Cu}^{\text{II}}\text{-Phen}_2$ (blue), $\text{Cu}^{\text{I}}\text{-Phen}_2$ (red, formed by the addition of ascorbate) and Cu-GSH (black) and a mixture of $\text{Cu}^{\text{II}}\text{-Phen}_2$ and GSH (green) at pH 7.4 (A) or 5 (B); C, D) Fourier Transforms (FT) moduli of the EXAFS of Cu-GSH (black) and the mixture of $\text{Cu}^{\text{II}}\text{-Phen}_2$ and GSH (green) at pH 7.4 (A) or 5 (B). Samples composition: $[\text{Cu}^{\text{II}}] = 1 \text{ mM}$, $[\text{Phen}] = 2 \text{ mM}$, $[\text{Asch}] = 10 \text{ mM}$ (for the Cu^{I} samples only), $[\text{GSH}] = 10 \text{ mM}$, glycerol 10 %, HEPES 100 mM pH 7.4 (A) or MES 100 mM pH 5 (B).

As $\text{Cu}^{\text{I}}\text{-Phen}_2$ shows absorption bands above 400 nm,^[18,34] we also recorded the UV-vis absorption spectra in order to further assess Cu-binding to Phen along the reaction. The appearance of a band at $\approx 420 \text{ nm}$ attributable to Cu^{I} bound to Phen was observed upon the addition of GSH at pH 5, while such a band did not appear when the reaction occurs at pH 7.4. In line with luminescence and XAS measurements, this further indicates that at pH 5 $\text{Cu}^{\text{II}}\text{-Phen}_2$ is reduced and at best partially dissociated by GSH, while most Cu^{II} is reduced and bound by GSH at pH 7.4 (Figure 3A, B). As Phen and GSH compete for Cu^{I} rather than Cu^{II} , we performed competition experiments between Phen and GSH for Cu^{I} under anaerobic conditions. In particular, we monitored by UV-vis spectroscopy the products of GSH addition to pre-formed $\text{Cu}^{\text{I}}\text{-Phen}_2$ (Figure 3C, D) and, *vice versa*, of the Phen addition to pre-formed $\text{Cu}^{\text{I}}\text{-GSH}$ (Figure S4A, B). In both cases, Cu^{I} complexes were formed by adding a $[\text{Cu}^{\text{I}}(\text{CH}_3\text{CN})_4]^+$ salt to a solution of GSH or Phen. At pH 7.4, the addition of GSH to the $\text{Cu}^{\text{I}}\text{-Phen}_2$ complex caused the disappearance of the band at $\approx 430 \text{ nm}$, commensurate with the dissociation of $\text{Cu}^{\text{I}}\text{-Phen}_2$ to form Cu-GSH . *Vice versa*, the band at 430 nm is not observed when Phen is added to Cu-GSH , confirming the higher stability of Cu-GSH clusters compared to $\text{Cu}^{\text{I}}\text{-Phen}_2$ (Figure S4A). At pH 5, the signal of $\text{Cu}^{\text{I}}\text{-Phen}_2$ does not disappear, but undergoes a slight shift upon addition of GSH, suggesting the formation of $\text{GS-Cu}^{\text{I}}\text{-Phen}$ ternary complexes (Figure 3D).^[18] A similar spectrum is observed when Phen is added to $\text{Cu}^{\text{I}}\text{-GSH}$ at pH 5 (Figure S4B).

Altogether, the spectroscopic characterization of the reaction mixture containing $\text{Cu}^{\text{II}}\text{-Phen}_2$ and GSH supports the hypothesis that lower dissociation of $\text{Cu}^{\text{II}}\text{-Phen}_2$ occurs at lysosomal pH, and hints at the formation of a ternary $\text{GS-Cu}^{\text{I}}\text{-Phen}$ complex, only detectable at pH 5 with 10 μM $\text{Cu}^{\text{II}}\text{-Phen}_2$ and 1 mM GSH.

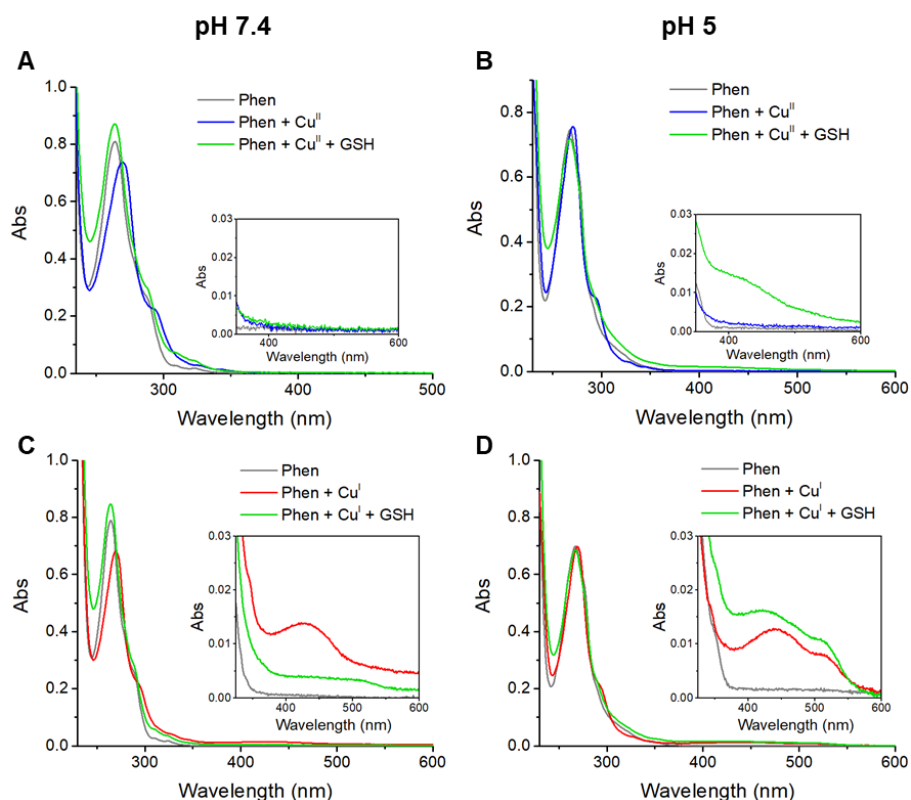


Figure 3. UV-vis absorption spectroscopy characterization of the reaction between Cu^{II}-Phen₂ and GSH (A, B) and of the competition between Phen and GSH for Cu^I under anaerobic conditions (C, D) at pH 7.4 (A, C) or 5 (B, D). In (C) and (D), Cu^I-Phen₂ was first formed by adding [Cu^I(CH₃CN)₄]⁺ to Phen, and then GSH was added. Sample composition: A, B) [Cu^{II}] = 10 μM, [Phen] = 25 μM, [GSH] = 1 mM, HEPES 100 mM pH 7.4 or MES 100 mM pH 5; C, D) [Cu^I] = 10 μM, [Phen] = 25 μM, [GSH] = 1 mM, HEPES 100 mM pH 7.4 or MES 100 mM pH 5.

Faster ROS formation and GSH oxidation catalysed by Cu-Phen₂ at lysosomal pH

Thus, we investigated the impact of such different pH-dependent speciation of Cu-Phen₂ on its capacity to generate ROS using GSH as the reductant. We evaluated the kinetics of HO[•] production by the Cu-Phen₂ complex in the presence of GSH at pH 7.4 and 5, by means of electron paramagnetic resonance (EPR) spectroscopy, using the nitroxyl radical 4-hydroxy-2,2,6,6-tetramethylpiperidin-1-oxyl (TEMPOL) as a spin scavenger. Indeed, the EPR signal of TEMPOL decreases over time upon reaction with radicals such as HO[•].^[35] At pH 5, the generation of HO[•] resulted to be ≈4-fold faster than at pH 7.4 (Figure 4A). Consistently, the aerobic GSH oxidation catalysed by Cu-Phen₂, which was monitored through the classical Ellmann's assay for thiols, also appeared to be ≈3-fold faster at pH 5 relative to pH 7.4 (Figure 4B).

Noteworthy, this trend is opposite to that of both "free" Cu^{II} with GSH,^[29] and Cu^{II}-Phen₂ in the presence of ascorbate as the reductant (Figure S5). Conversely, some of us recently reported a similar pH-dependent behaviour for a Cu-thiosemicarbazone complex (Cu-Dp44mT),^[29] whose catalytic mechanism involves protonation of the ligand that cannot be at play in this case (due to the absence of protonable groups in Cu-Phen₂).

Remarkably, Cu-Phen₂ was more than 100 times faster in GSH oxidation than Cu-Dp44mT under similar conditions.^[16,36]

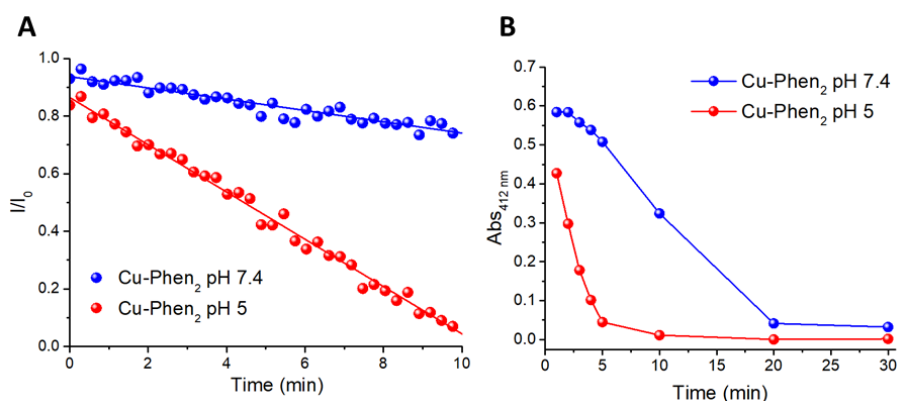


Figure 4. HO[•] production (A) and GSH oxidation (B) catalysed by Cu-Phen₂ at pH 7.4 (blue) or 5 (red). To measure GSH oxidation (B), aliquots were taken from the reaction mixture at several time points and transferred to the assay mixture composed of 100 μM DTNB and 1 mM EDTA in 50 mM TRIS buffer pH 8.2. Samples composition: [Cu^{II}] = 10 μM, [Phen] = 25 μM, [GSH] = 1 mM, buffer: HEPES 100 mM pH 7.4 or MES 100 mM pH 5; in (A), [TEMPO]₀ = I₀ = 20 μM.

DFT calculations of the catalytic mechanism leading to HO[•] production

To get insights into the mechanism of HO[•] production and GSH oxidation catalysed by the Cu-Phen₂ complex, we carried out DFT calculations to study the series of reactions and the identity of the species taking part in the catalytic redox cycle. In order to reduce the computational effort, L-cysteine (Cys) was used as a thiol model instead of GSH. The proposed reduction pathway is drawn in Figure 5. A more detailed description, together with the energy profiles and the DFT fully optimized geometrical structures of stationary points located along the entire reaction pathway are reported in the SI. The whole redox cycle involves four main steps: i) the reduction of the Cu^{II}-Phen₂ complex by Cys entailing the release of one of the Phen ligands (Figure 5A); ii) the re-oxidation of the Cu^I complex by dioxygen leading to the formation of superoxide bound to Cu^{II} (Figure 5B); iii) the formation of the H₂O₂ molecule bound to the metal centre assisted by hydronium units as protonating agents (Figure 5C); iv) the subsequent production of the hydroxyl radical HO[•] from the hydrogen peroxide complex assisted by both Cys⁻ and hydronium units (Figure 5D).

The first step, which provides the reduction of the Cu^{II}-Phen₂ complex by Cys, starts from the CuPhen₂(H₂O) complex, which, in agreement with X-ray analysis,^[37] presents a five-coordinate distorted trigonal bipyramid geometry. Formation of Cu^I centre goes through the formation of a six-coordinate octahedral complex intermediate (²[Int1]⁺), as a consequence of the coordination of Cys to the Cu^{II}. The interaction of the formed complex with a second Cys⁻ unit (²[Int2]⁺) allows the reduction of Cu^{II} by an inner-sphere mechanism in which the second Cys⁻ forms a S-S interaction with the bound Cys. Then the second Cys transfers an electron to the Cu^{II} centre via the bound Cys acting as an electron relay (TS1). The reduction and the simultaneous release of one of the Phen ligands leads to the formation of the final product that assumes a distorted tetrahedral geometry, whose spin density distribution analysis confirms the unpaired electron localized on the unbound Cys.

For the reaction to proceed to the second step, very numerous attempts have been made to establish the possible ways in which O₂ can bind to the formed [Cu^IPhen(H₂O)(Cys)] complex. The most reliable pathway implies the overcoming of an energy barrier in which the O₂ molecule approaches the complex establishing a new bond and one electron is transferred from Cu^I to O₂ upon binding (TS2 in Figure 5B). The spin density distribution analysis on the formed complex confirms that the two unpaired electrons are localized on the Cu^{II} centre and oxygen. A geometrical rearrangement takes place and leads to the formation of a five-coordinate end-on superoxide complex in a triplet state.

Once the superoxide bound to Cu^{II} is formed, the reaction continues with the formation of the H₂O₂ molecule bound to the metal centre. Several mechanistic hypotheses were explored, and the most reliable pathway involves two H₃O⁺ units as protonating agents (Figure 5C). When a H₃O⁺ moiety comes close to the ³[Cu^{II}Phen(H₂O)(Cys)O₂⁻] a proton transfer to the distal oxygen atom of the bound superoxide spontaneously occurs (³[Int3]⁺). A successive proton shift from a second hydronium ion takes place together with the spontaneous transfer of one electron from the bound deprotonated Cys to the

proximal oxygen atom of superoxide allowing the formation of the hydrogen peroxide molecule that remains bound to the metal centre. This transformation is accompanied by the formation of the radical cysteine, Cys[•]. The analysis of the spin density of the formed complex confirms how the unpaired electrons are distributed, that is on the sulphur atom and Cu^I ion.

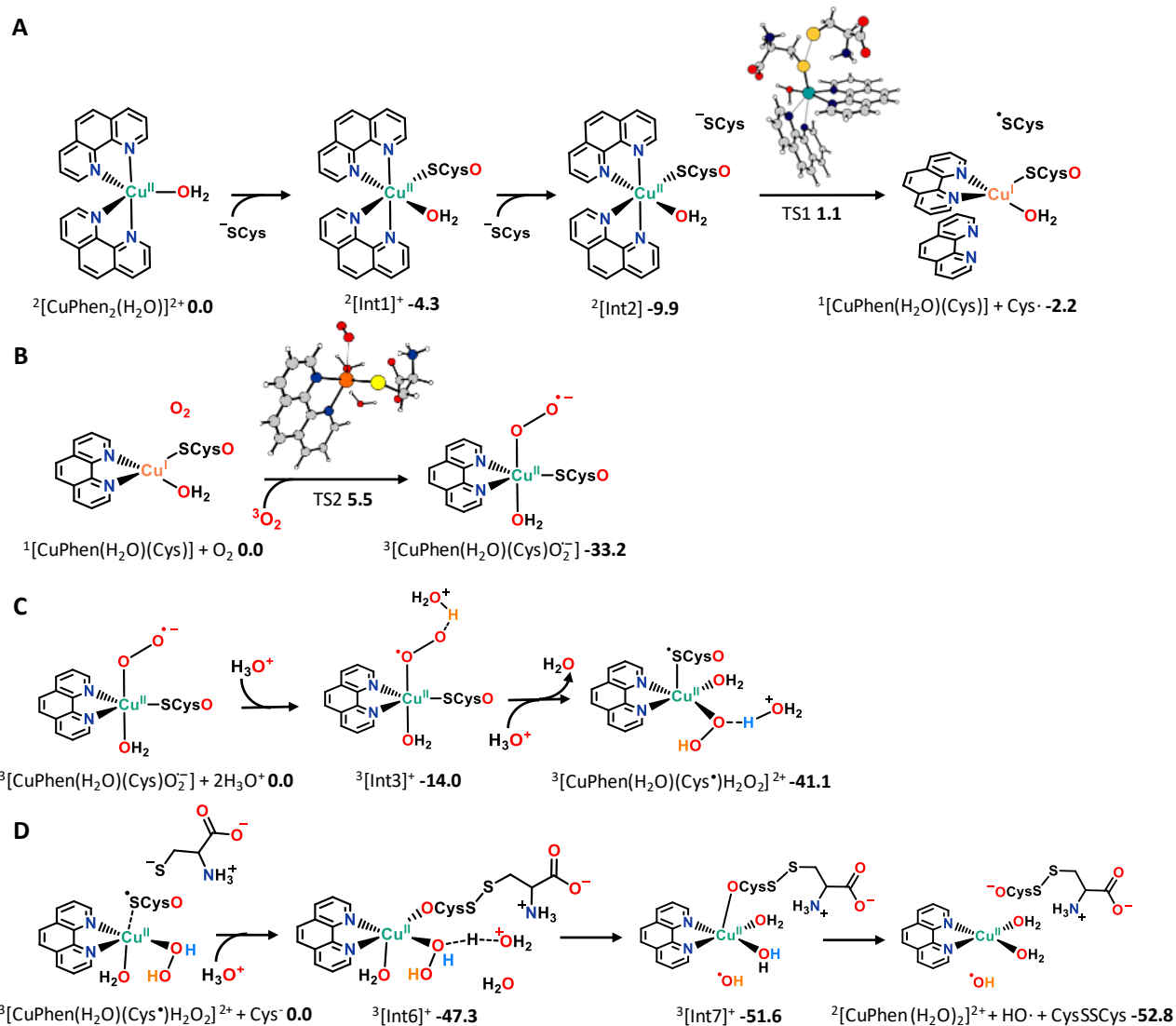


Figure 5. DFT-calculated mechanism of a) $\text{CuPhen}_2(\text{H}_2\text{O})$ reduction in the presence of two deprotonated Cys, b) binding of O_2 to the Cu^I complex $[\text{CuPhen}(\text{H}_2\text{O})(\text{Cys})]$, c) the consecutive protonation of distal and proximal oxygen atoms of the O_2 molecule bound to the Cu^{II} complex ${}^3[\text{Cu}^{\text{II}}\text{Phen}(\text{H}_2\text{O})(\text{Cys})\text{O}_2]^-$ to form H_2O_2 and formation of hydroxyl radicals as a consequence of the protonation of the proximal oxygen of the bound H_2O_2 molecule by d) a third hydronium ion assisted by the transfer of one electron from an additional Cys. The relative Gibbs free energies ($\Delta G^{298\text{K}}$), calculated with respect to the sum of the energies of separated reactants set as zero reference energy, are in kcal mol^{-1} .

The final production of the hydroxyl radical HO^\bullet from the formed hydrogen peroxide molecule bound to the Cu^{II} centre is assisted by a second Cys[•] unit and occurs thanks to the intervention of another hydronium ion as protonating agent (Figure 5D). Once again, electron transfer occurs by an inner-sphere mechanism as the approaching Cys[•] donates an electron to the complex forming a S-S interaction with the bound Cys and leads to the coupling of the two formed thiyl radicals in the form of oxidized cysteine, CysSSCys (${}^3[\text{Int6}]^+$). At the same time, the hydronium ion protonates the proximal oxygen of the bound H_2O_2 molecule causing the cleavage of the O-O bond and the release of the HO^\bullet radical (${}^3[\text{Int7}]^+$). The last step involves the release of the CysSSCys ligand and allows the regeneration of the Cu^{II} complex, bearing a Phen and two water ligands, which can restart the redox cycle.

Since the identity of the complex re-entering the catalytic cycle, which bears only one Phen ligand, is different with respect to that of the Cu^{II}-Phen₂ complex initially involved, calculations were performed in order to verify how the course of the Cu^{II} reduction reaction changes. The reaction requires the intervention of two Cys⁻ units to occur and requires the overcoming of a rather low energy barrier. Further details can be found in the SI. It is worth mentioning that with respect to the Cu^{II} reduction taking place at the first cycle, all the stationary points lie below the zero reference energy of separated reactants and the height of the barrier for the transition state is about one-half of that involved in the first cycle. Once formed, the Cu^I complex [Cu^IPhen(H₂O)(Cys)] can be re-oxidized by dioxygen as shown in Figure 5B and, then, the cycle can continue with the next steps leading to the production of hydroxyl radicals.

Role of lysosomal acidification on the cytotoxicity of Cu-Phen₂

Finally, since lysosomal pH enhanced the rate of ROS formation and GSH oxidation catalysed by Cu-Phen₂, we investigated whether lysosomal acidification could influence the anticancer activity of Cu-Phen₂. To assess this, we employed the H⁺-pump inhibitor bafilomycin A1 (Baf A1), known to impede lysosomal acidification,^[38] in combination with Cu^{II}-Phen₂ (Figure 6). In more detail, we subjected human colon cancer cells SW480 to pre-treatment with varying concentrations of Baf A1 (ranging from 0 to 5 nM) for one hour. Subsequently, Cu^{II}-Phen₂ was added to the Baf A1-treated cells in concentrations up to 2.5 μM (Figure 6A), avoiding concentrations exceeding 5 μM, as they already induce profound cell death (Figure S12). Parallel experiments with reference compounds, namely Phen, CuSO₄, and cisplatin, were conducted following the same procedure (Figure 6B, D). After 48 hours of drug combination exposure, we assessed cell viability using an MTT-based assay. Given the crucial role of lysosomes in cell viability, the extended exposure period of 48 hours with Baf A1 exerted a discernible impact in cell viability. In accordance to the literature,^[29,39,40] this exposure led to up to a 75% reduction in cell viability at the highest concentration (Figure 6). Concerning the combined effects, Baf A1 consistently diminished the anticancer activity of Cu-Phen₂ across all concentrations (Figure 6A), thus revealing an antagonistic impact of lysosomal de-acidification on the anticancer activity of Cu-Phen₂. In contrast, the reference compounds exhibited an anticipated additive (for Phen and cisplatin) or no effect (for CuSO₄) (Figure 6B-D). These outcomes provide a seminal indication that the acidic pH within lysosomes could be pivotal for the cytotoxicity of Cu-Phen₂.

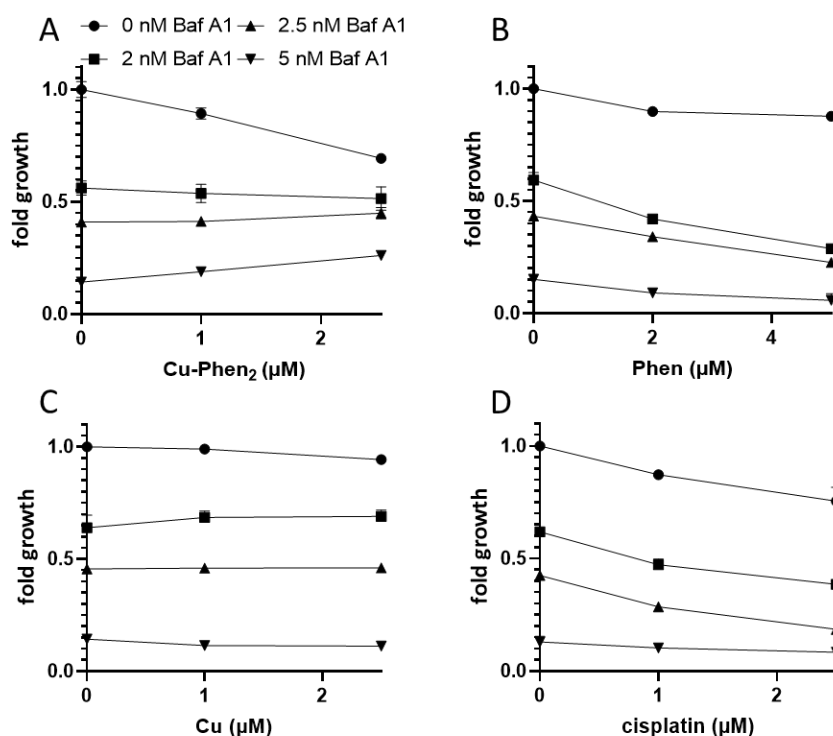


Figure 6. Effect of bafilomycin A1 (Baf A1) on viability of SW480 cells treated with Cu-Phen₂ (A) with indicated concentrations for 48 h. Phen (B), CuSO₄ (C) and cisplatin (D) were used as references. Viability was measured by an MTT-based viability assays. Values given are mean \pm SD derived from triplicates of one representative experiment out of three and normalized to untreated.

Correlation between GS-Cu^I-Phen population and pro-oxidant activity

The outstanding capacity of the Cu-Phen₂ complexes to catalyse the formation of ROS in the presence of a reductant such as ascorbate or GSH has long been recognised and used to induce oxidative stress and cell death for anticancer purposes.

However, biological thiols such as GSH and metallothioneins are strong de-activators of Cu-Phen₂ at pH 7.4.^[16,17]

Here, we showed for the first time that Cu-Phen₂ retains instead higher stability against GSH at lysosomal pH (Figure 1-3), due to decreased Cu^I-GSH affinity (see SI). This correlates with a faster generation of ROS and GSH oxidation at lysosomal pH relative to pH 7.4, as demonstrated by EPR spin scavenging experiments and the DTNB assay, respectively (Figure 4). This behaviour is remarkable since Cu-catalysed thiol oxidation is generally faster at higher pH.

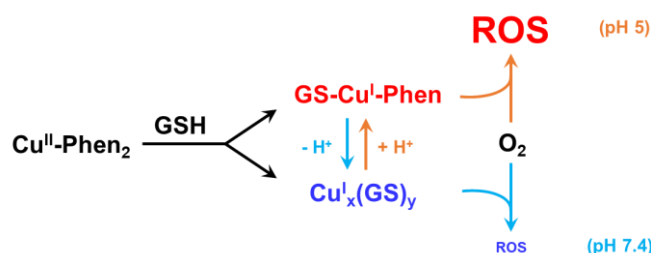
The quantum mechanical analysis reported shed light on the mechanistic aspects of the process. The identified pathway suggests the involvement of a ternary GS-Cu^I-Phen intermediate formed when added Cys, used as a model for GSH, displaces one of the Phen ligands, causing the reduction of Cu^{II} to Cu^I and the oxidation of the thiol to a thiyl radical. Cu^I re-oxidation takes place as a consequence of the binding of dioxygen to the formed ternary complex.

The formation of such a ternary GS-Cu^I-Phen intermediate complex was corroborated experimentally by UV-vis spectroscopy and is further confirmed by a quantitative XAS analysis. Indeed, the EXAFS spectrum of the reaction mixture at pH 5 (Figure 2D) can be fitted with the DFT-optimized structure of the Cu^IPhen(H₂O)(Cys) (Figure 5A), obtaining a good agreement between the model and the experimental data (Figure S10 and Table S4). Besides, in the XAS spectrum of Cu^{II}-Phen₂ and GSH at pH 7.4, as pointed out above, the appearance of a Cu-Cu peak at about 2.8 Å in the FT (Figure 2C) suggests the partial formation of Cu^I-GSH clusters. Hence, we tried to fit the spectrum of Cu^{II}-Phen₂ and GSH at pH 7.4 as the linear combination of the spectrum of the ternary mixture at pH 5, corresponding to the ternary GS-Cu^I-Phen complex, and the spectrum of Cu^I-GSH at pH 7.4. Interestingly, both the XANES and EXAFS spectra of the ternary mixtures

are very well reproduced by such a linear combination of GS-Cu^I-Phen (spectrum Cu^{II}-Phen₂ + GSH pH 5) and Cu^I-GSH (spectrum Cu-GSH pH 7.4) in about 1:1 ratio (Figure S11). Hence, under the experimental conditions of XAS (i.e. millimolar Cu-Phen₂ concentration and low, 10-fold, GSH excess), the ternary species appears to be predominant at pH 5, but also present at pH 7.4.

On the contrary, under catalytic conditions (micromolar Cu^{II}-Phen₂ concentration and high, 100-fold, GSH excess) no Cu^I bound to Phen could be detected at pH 7.4 (Figure 3A), although a much higher activity than free Cu^{II} was observed in line with previous reports.^[16] This suggests that the ternary intermediate is also formed, at least transiently, at pH 7.4, but very low populated (below detection levels), underscoring its outstanding capacity in O₂ reduction.

Hence, the balance between the pro-oxidant GS-Cu^I-Phen ternary complex and the relatively redox-inert Cu^I-GSH clusters determines the different reactivity at different pH values. Indeed, as Cu^I-GSH is a poor catalyst of ROS production compared to GS-Cu^I-Phen, the reaction is faster when less Cu^I-GSH is formed, that is at lower pH (Scheme 2).



Scheme 2. As suggested by spectroscopic measurements and DFT calculations, two main species are formed upon the reaction of Cu^{II}-Phen₂ with GSH, namely the ternary GS-Cu^I-Phen complex and Cu^I_x(GS)_y clusters. At lower pH, the formation of ternary GS-Cu^I-Phen is favoured due to the lower affinity of GSH for Cu. As a result, the rate of ROS production results to be higher at lower pH.

Conclusions

In this study, unprecedented evidence is provided that a ternary GS-Cu^I-Phen species, and not the starting Cu^{II}-Phen₂ complex, is accountable for its pro-oxidant, and possibly cytotoxic, activity. Due to the reduced affinity of GSH for Cu^I, this ternary species is more populated at the acidic pH of lysosomes, resulting in faster HO[•] production. This explains the role of lysosomal acidification on the cytotoxic activity of Cu-Phen₂, reported here for the first time. The pH-dependent behaviour shown here for Cu-Phen with GSH could be likely shared by other chelators that have a high affinity for Cu^I, and hence escape the dissociation by GSH at acidic pH. The possibility of forming ternary species with GSH as the most active species might also be a more general feature. Moreover, our findings spotlight lysosomal targeting as an innovative strategy to improve the efficacy of Cu-based drugs.

Acknowledgements

We thank Alex Kress and Dr Alice Santoro for preliminary results and the European Synchrotron Radiation Facility (ESRF) for the provision of synchrotron radiation facilities under proposal number LS-3102. E.F. acknowledges financial support from the French National Research Agency (ANR) through the CHAPCOP-ANR-19-CE44-0018 program. This research has been supported by MUR, Autorità di Gestione PON "Ricerca e Innovazione" 2014–2020 (CCI 2014IT16M2OP005) and Università della Calabria. H.S. was financed by the Austrian Science project FG3 (awarded to P.H.). S.M. and F.S. acknowledge financial support from the "PANDA" project, University of Rome Tor Vergata and BIOPHYS, INFN. The FAME project is financially supported by the French "grand emprunt" EquipEx (MAGNIFIX, ANR-21-ESRE-0011), the French "Programmes et équipements prioritaires de recherche" (DIADEM), the CEA-CNRS CRG consortium and the INSU CNRS institute.

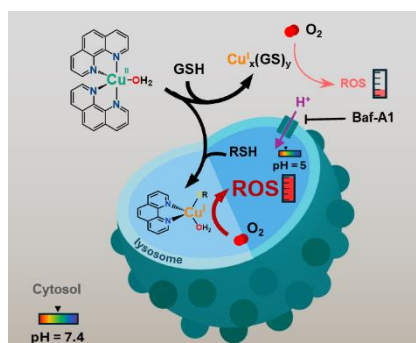
References

- [1] M. A. Zoroddu, J. Aaseth, G. Crisponi, S. Medici, M. Peana, V. M. Nurchi, *J. Inorg. Biochem.* **2019**, *195*, 120–129.
- [2] S. G. Kaler, *Am. J. Clin. Nutr.* **1998**, *67*, 1029S-1034S.
- [3] E. J. Ge, A. I. Bush, A. Casini, P. A. Cobine, J. R. Cross, G. M. DeNicola, Q. P. Dou, K. J. Franz, V. M. Gohil, S. Gupta, S. G. Kaler, S. Lutsenko, V. Mittal, M. J. Petris, R. Polishchuk, M. Ralle, M. L. Schilsky, N. K. Tonks, L. T. Vahdat, L. Van Aelst, D. Xi, P. Yuan, D. C. Brady, C. J. Chang, *Nat. Rev. Cancer* **2022**, *22*, 102–113.
- [4] V. C. Shanbhag, N. Gudekar, K. Jasmer, C. Papageorgiou, K. Singh, M. J. Petris, *Biochim. Biophys. Acta - Mol. Cell Res.* **2021**, *1868*, 118893.
- [5] D. Denoyer, S. Masaldan, S. La Fontaine, M. A. Cater, *Metallomics* **2015**, *7*, 1459–1476.
- [6] A. Gupte, R. J. Mumper, *Cancer Treat. Rev.* **2009**, *35*, 32–46.
- [7] P. Tsvetkov, S. Coy, B. Petrova, M. Dreishpoon, A. Verma, M. Abdusamad, J. Rossen, L. Joesch-Cohen, R. Humeidi, R. D. Spangler, J. K. Eaton, E. Frenkel, M. Kocak, S. M. Corsello, S. Lutsenko, N. Kanarek, S. Santagata, T. R. Golub, *Science* **2022**, *375*, 1254–1261.
- [8] V. Oliveri, *Front. Mol. Biosci.* **2022**, *9*, 1–14.
- [9] P. Lelièvre, L. Sancey, J. L. Coll, A. Deniaud, B. Busser, *Cancers (Basel)*. **2020**, *12*, 1–25.
- [10] S. Hager, K. Korbula, B. Bielec, M. Grusch, C. Pirker, M. Schosserer, L. Liendl, M. Lang, J. Grillari, K. Nowikovsky, V. F. S. Pape, T. Mohr, G. Szakács, B. K. Keppler, W. Berger, C. R. Kowol, P. Heffeter, *Cell Death Dis.* **2018**, *9*, 1052.
- [11] C. Marzano, M. Pellei, F. Tisato, C. Santini, *Anticancer. Agents Med. Chem.* **2012**, *9*, 185–211.
- [12] C. Santini, M. Pellei, V. Gandin, M. Porchia, F. Tisato, C. Marzano, *Chem. Rev.* **2014**, *114*, 815–862.
- [13] F. Tisato, C. Marzano, M. Porchia, M. Pellei, C. Santini, *Med. Res. Rev.* **2010**, *30*, 708–749.
- [14] D. Denoyer, S. A. S. Clatworthy, M. A. Cater, in *Met. Dev. Action Anticancer Agents*, Met Ions Life Sci, **2018**, pp. 469–506.
- [15] U. Jungwirth, C. R. Kowol, B. K. Keppler, C. G. Hartinger, W. Berger, P. Heffeter, *Antioxidants Redox Signal.* **2011**, *15*, 1085–1127.
- [16] K. Kobashi, *BBA - Gen. Subj.* **1968**, *158*, 239–245.
- [17] A. Santoro, J. S. Calvo, M. D. Peris-Díaz, A. Krężel, G. Meloni, P. Faller, *Angew. Chemie - Int. Ed.* **2020**, *59*, 7830–7835.
- [18] B. C. Gilbert, S. Silvester, P. H. Walton, *J. Chem. Soc. Perkin Trans. 2* **1999**, 1115–1121.
- [19] D. S. Sigman, D. R. Graham, V. D'Aurora, A. M. Stern, *J. Biol. Chem.* **1979**, *254*, 12269–12272.
- [20] S. Masuri, P. Vaňhara, M. G. Cabiddu, L. Moráň, J. Havel, E. Cadoni, T. Pivetta, *Molecules* **2022**, *27*, 49.
- [21] C. Lüdtke, S. Sobottka, J. Heinrich, P. Liebing, S. Wedepohl, B. Sarkar, N. Kulak, *Chem. - A Eur. J.* **2021**, *27*, 3273–3277.
- [22] L. Ruiz-Azuara, G. Bastian, M. E. Bravo-Gómez, R. C. Cañas, M. Flores-Alamo, I. Fuentes, C. Mejia, J. C.

- García-Ramos, A. Serrano, *Cancer Res.* **2014**, *74*, CT408–CT408.
- [23] X. Cai, N. Pan, G. Zou, *BioMetals* **2007**, *20*, 1–11.
- [24] R. Alemón-Medina, J. L. Muñoz-Sánchez, L. Ruiz-Azuara, I. Gracia-Mora, *Toxicol. Vitr.* **2008**, *22*, 710–715.
- [25] P. Nunes, I. Correia, F. Marques, A. P. Matos, M. M. C. Dos Santos, C. G. Azevedo, J. L. Capelo, H. M. Santos, S. Gama, T. Pinheiro, I. Cavaco, J. C. Pessoa, *Inorg. Chem.* **2020**, *59*, 9116–9134.
- [26] S. Hager, V. F. S. Pape, V. Pósa, B. Montsch, L. Uhlík, G. Szakács, S. Tóth, N. Jabronka, B. K. Keppler, C. R. Kowol, É. A. Enyedy, P. Heffeter, *Antioxidants Redox Signal.* **2020**, *33*, 395–414.
- [27] A. G. Ritacca, E. Falcone, I. Doumi, B. Vileno, P. Faller, E. Sicilia, *Inorg. Chem.* **2023**, *62*, 3957–3964.
- [28] E. Falcone, F. Stellato, B. Vileno, M. Bouraguba, V. Lebrun, M. Ilbert, S. Morante, P. Faller, *Metallomics* **2023**, *15*, mfad040.
- [29] E. Falcone, A. G. Ritacca, S. Hager, H. Schueffl, B. Vileno, Y. El Khoury, P. Hellwig, C. R. Kowol, P. Heffeter, E. Sicilia, P. Faller, *J. Am. Chem. Soc.* **2022**, *144*, 14758–14768.
- [30] D. L. Pountney, I. Schauwecker, J. Zarn, M. Vašák, *Biochemistry* **1994**, *33*, 9699–9705.
- [31] M. T. Morgan, L. A. H. Nguyen, H. L. Hancock, C. J. Fahmi, *J. Biol. Chem.* **2017**, *292*, 21558–21567.
- [32] M. J. Stillman, Z. Gasyna, *Methods Enzymol.* **1991**, *205*, 540–555.
- [33] L. S. Kau, D. J. Spira-Solomon, J. E. Penner-hahn, K. O. Hodgson, E. I. Solomon, *J. Am. Chem. Soc.* **1987**, *109*, 6433–6442.
- [34] J. M. Vaal, K. Mechant, R. L. Rill, *Nucleic Acids Res.* **1991**, *19*, 3383–3388.
- [35] K. Takeshita, K. Saito, J. I. Ueda, K. Anzai, T. Ozawa, *Biochim. Biophys. Acta - Gen. Subj.* **2002**, *1573*, 156–164.
- [36] I. Doumi, L. Lang, B. Vileno, M. Deponete, P. Faller, *Chem. – A Eur. J.* **2024**, *30*, e202304212.
- [37] H. Nakai, Y. Noda, *Bull. Chem. Soc. Jpn.* **1978**, *51*, 1386–1390.
- [38] T. Yoshimori, A. Yamamoto, Y. Moriyama, M. Futai, Y. Tashiro, *J. Biol. Chem.* **1991**, *266*, 17707–17712.
- [39] Y. C. Wu, W. K. K. Wu, Y. Li, L. Yu, Z. J. Li, C. C. M. Wong, H. T. Li, J. J. Y. Sung, C. H. Cho, *Biochem. Biophys. Res. Commun.* **2009**, *382*, 451–456.
- [40] Y. Yan, K. Jiang, P. Liu, X. Zhang, X. Dong, J. Gao, Q. Liu, M. P. Barr, Q. Zhang, X. Hou, S. Meng, P. Gong, *Sci. Rep.* **2016**, *6*, 1–13.

Entry for Table of Content

The Cu^{II} -Phen₂ complex evolves in the presence of glutathione (GSH) forming mostly Cu^{I} -GSH clusters and minor GS- Cu^{I} -Phen species responsible for the prooxidant activity. The higher population of this species at the acidic pH of lysosomes fastens GSH oxidation and reactive oxygen species (ROS) formation *in vitro*. Consistently, the inhibition of lysosomal acidification by bafilomycin A1 (Baf-A1) decreases the cytotoxicity of Cu-Phen₂ in cancer cells.



Twitter/X:

[@BiochemMetal](https://twitter.com/BiochemMetal)

[@PROMOCSlab](https://twitter.com/PROMOCSlab)

[@EnriFalc1](https://twitter.com/EnriFalc1)